Supplementary Materials for

Convergent Evolution Between Insect and Mammalian Audition

Fernando Montealegre-Z.,* Thorin Jonsson, Kate A. Robson-Brown, Matthew Postles, Daniel Robert*

*To whom correspondence should be addressed. E-mail: fmontealegrez@lincoln.ac.uk (F.M.-Z.); d.robert@bristol.ac.uk (D.R.)

Published 16 November 2012, *Science* **338**, 968 (2012)
DOI: 10.1126/science.1225271

This PDF file includes:

Other Supplementary Material for this manuscript includes the following:
(available at www.sciencemag.org/cgi/content/full/338/6109/968/DC1)

Materials and Methods

Experimental animals

We used 21 individuals (10 males and 11 females) of *Copiphora gorgonensis* (Tettigoniidae, Copiphorini), a species endemic to the island of Gorgona, Colombia National Natural Park (PNN) (*6*). PNN Gorgona is a small island with an area of 13.3 km^2, situated in the southwest coast of Colombia (lat 2°47', 3°6' N; long 78°6', 78°18' W). Specimens were collected as nymphs in their natural habitat in November 2009 and maintained in captivity until they reached adulthood.

An unusual song structure

Males call females in the low ultrasonic range using a sequence of short duration pure-tone pulses, each lasting ca. 8 ms (*6*). Each pulse is composed of two distinct parts, starting with a very stable constant frequency (23kHz± 0.62 kHz, n=10) lasting 4 ms, followed by a 4-ms frequency modulation from 23-18 kHz (Fig. 1). This acoustic structure is somewhat usual in insects, and is reminiscent of the calls of some male frogs occupying a similar sensory ecological niche (*21*).

Morphological studies of the auditory system

In addition to optical microscopy, the auditory anatomy of the katydid was examined using X-ray micro computer tomography (μ-CT) and 3D reconstruction using standard biomedical imaging software (AMIRA v.5.3). The X-ray images were obtained using a SkyScan 1172 micro-CT scanner (SkyScan, Kontich, Belgium). First a general scan of the forelegs and thorax area was run to establish the general anatomy of the auditory system and associated tracheal tubes (fig. S1A and B). Second, a high resolution scan of the proximal part of the tibia was performed to reveal the detailed anatomy of the tympanal organ (fig. S1C and D). For the general anatomy of the acoustic trachea and ears, animals were scanned at 100 kV, 36 μA and with a 0.5 mm thick aluminum filter. The object stage rotated through 180º in increments of 1.5º. The general scans were undertaken with a resolution of 10.9 μm^3 voxel size and obtained with a four-part oversize scan with camera offset. This yielded a time of reconstruction of 1. 818s per X-ray slice. The detailed scans of the auditory organ were done at higher resolution (2.8 μm^3 voxel size) to reveal internal 3D morphology in unprecedented clarity (see Fig. 2 in the main text, and fig. S1 C and D). The raw micro-CT data was reconstructed using

(NRecon, v. 1.6.1.5, SkyScan, Kontich, Belgium) on a cluster of four networked PCs. The resulting 2D images were processed using CTan (CTan, v. 1.9.2.5, SkyScan, Kontich, Belgium) in order to segment the trachea and air space contained and to create 3D rendering of the trachea that were then visualized using CTVol, v. 2.2.0.0, SkyScan, Kontich, Belgium).

Using high resolution scans, the tibia of the earless mesothoracic leg was also examined to compare it with that of the prothoracic leg. Anatomical differences between pro and mesothoracic legs reveal the extent of auditory specializations (compare figs. S1C and D and fig. S2).

3D models were constructed with AMIRA 5.3 software (Visage Imaging, Inc. San Diego, CA, USA). The 3D voxel data were segmented by separating the regions of interest from the background. Measurements of the structures of interest (lengths and volume rendering) were also done in AMIRA using the Voltex tool and statistics modulus.

Measuring the mechanical response of the auditory system

Tympanal vibrations in response to sound (fig. S3) were studied using two different acoustical methods: 1) The auditory system was actuated using an acoustic free-field, exposing it to natural acoustic conditions, with sound impinging the tympanal membranes directly and through their tracheal input (fig. S4 A), or 2) direct external and internal acoustic inputs were provided independently using a confined acoustic field (fig. S4 B).

In the first method, specimen were exposed to a free acoustic field, following previously developed protocols (*22*). The animal holder was positioned on a vibration-isolation air table along with the microscanning laser Doppler vibrometer (LDV; Polytec PSV-300-F; Waldbronn, Germany). A loudspeaker (ACR, FT 17H,

Horn Tweeter, Fostex, Tokyo, Japan) was positioned 30 cm away, ipsilateral to the ear examined, playing periodic chirps in the range of 5-50 kHz. Computer controlled spectral correction of the acoustic analytical signals was used to maintain a constant sound level (±1.5 dB maximum deviation) across the

complete range of frequencies, measured at the ipsilateral spiracle using a 1/8" (3.2 mm) precision pressure microphone (Bruel & Kjaer, 4138; Nærum, Denmark) and a preamplifier (Bruel & Kjaer, 2633). The microphone's sensitivity was calibrated using a

sound level calibrator (Bruel & Kjaer, 4231). Broadband sound stimulation was played at 80 dB SPL re. 20 μPa, produced with a sampling frequency of 512 kHz by the PSV 300 internal data acquisition board (National Instruments PCI-4451; Austin, TX, USA), amplified (Sony Amplifier Model TAFE570; Tokyo, Japan) and passed to the loudspeaker. The vibration velocity of the tympanal membranes was measured using the LDV with an OFV-056 scanning head fitted with a close-up attachment. The laser spot with this setup was ca. 5 μm in diameter, and the beam was spatially positioned with an accuracy of ca. 1 μm. The mechanical responses were analyzed by simultaneously recording the vibration velocity of the auditory structures, and the sound stimulus measured either at the auditory organ or at the auditory spiracle. The laser scanner was used to monitor vibrations along a transect of nearly 400μm, covering slightly more that the entire length of the auditory system (fig. S6). These data enabled us to calculate magnitude and phase frequency transfer functions, providing essential information on the vibrational behavior of different auditory structures. Time data were also obtained to examine the system's response to single frequencies. Frequency and time-resolved data were acquired at either 512 kHz or at 1.28 MHz sampling rates.

In the species studied here, as in many other Copiphorini, the tympanal membranes are partially occluded by protective cuticular flaps (Figs. 2, and fig. S1 C). Therefore, the laser beam had to be directed through the tympanal slits in order to leave these flaps intact.

Since the laser spot position was monitored via a live video feed to the vibrometer's controlling computer, the surface area of the tympanal membranes could be scanned with high spatial accuracy, each scanning lattice including 800-1200 measurement points. The PSV300 LDV system enabled the recording of tympanal motion in non-contact non-loading condition, e.g., without placing reflective glass particles on the membrane surface. However, as is often the case with LDV, the laser beam cannot be always perfectly perpendicular to the membrane and its vector of motion, so exact quantification of the absolute vibration magnitude cannot be drawn. This does not affect frequency and phase information, or relative measurements used to compare different treatments with each other.

After some recordings, as a control procedure, the tympanal flaps were partially removed to allow for a perpendicular projection of the laser beam on the membrane surface and associated structures. This procedure allowed to accurate positioning of 1200-2000 scanning points on the whole tympanal system. Quality control analysis confirmed in all cases (n=21) that the frequency and phase response of the tympanal membrane (TM) and tympanal plate (TP) did not change after alteration of the cuticular flaps (fig. S3A to D). As expected, vibration velocities were higher with a normal angle of incidence between the laser beam and the scanned surface, yet phase relationships remained unchanged. By removing the tympanal flaps we gained complete access to the TPs. These recordings show that the TPs exhibit similar spectral properties to the TMs, but importantly vibrate with opposite phase (Fig. S3E and F).

Using the same preparation (before and after flap ablation), the tympana were also stimulated with 4-cycle pulses at frequencies ranging from 5 kHz to 50 kHz, in increments of 5 kHz steps, and with sound pressure of 1 Pa (peak to peak) (=94 dB SPL). The analytical signals were produced by a function generator (Agilent 33120A, 15MHz Function/Arbitrary waveform generator, Agilent Technologies UK Ltd., Edinburgh, UK), 1 and 4 cycle bursts at specific frequencies, with a burst rate of 50 Hz, and 500 mV peak to peak amplitude. The function generator was synchronized with the PSV 300 internal data acquisition board, using its TTL trigger port. Stimulus amplitudes were controlled and measured via the amplifier, step attenuator see Windmill et al. (*19*) and monitoring pressure microphones, as described above.

Time-resolved vibrations were measured from the anterior and posterior tympanal membrane (ATM, PTM), as well as from the dorsal cuticle separating both tympanal membranes (figs. S1C, S5, S6). The position of the LDV scanning unit was adjusted to obtain optical access to both ATM and PTM, leaving the specimen's position and sound field unchanged during the procedure. The temporal resolution of all time-resolved recordings was 1.2 μs.

To summarize, in this first set of experiments broadband signals and single tones at different frequencies were intended to study both tympanal and cuticular vibrations when the specimen was exposed to sound in a free acoustic field.

The second method was developed to test whether sound-induced vibrations recorded through the dorsal cuticle (see fig. S5) were the product of adequate auditory function or of artifact leg resonances produced by inappropriate acoustic conditions. Specimens were mounted on a custom build platform that allows for the effective acoustic isolation of the two main sound inputs (tympanum vs. spiracle) of the katydid ear (fig. S4 B and C). This device consists of a metallic frame (10 cm X 10 cm) that allows the assembling of two panels (Perspex, 5 cm X 10 cm X 1 mm), one fitted on top of the other. The ventral panel holds a small body holder, while the one on top has a central notch that accommodates the insect's neck and two holes placed on each side of the neck notch; these holes embrace the forelegs at the femora (fig. S4 B). The specimen was anesthetized with CO_2, then its legs and head were fitted into the respective holes of the upper panel and carefully inserted into the metallic frame. This way, head and forelegs are on one side of the joint panels, while the meso- and meta- thoraces (mid and hind legs) and the auditory spiracle are on the other side. This arrangement results in the two acoustic inputs, the tympanum and the spiracle, to be acoustically isolated (fig. S4B and C). The converging edges of the two panels, and small gaps surrounding legs and neck are sealed using liquid latex (Magnacraft, Midhurst, UK). Mid and hind legs were fixed to the body holder with Blu-Tack® (Bostik-Findley, Stafford, UK). The procedure is reversible and imparts no injury to the animal.

Sound was delivered at the spiracle using a custom build probe loudspeaker. As the probe loudspeaker offers high acoustic impedance, the surface area of the separation panel is sufficient to create an effective acoustic barrier, in effect allowing sound to be delivered either to the TMs or the auditory spiracle.

Probe loudspeaker design and calibration

The probe loudspeaker consisted of a tube attached to a dome-like plastic piece fitted on the cone of a loudspeaker (ACR, FT 17H, described before). The dome-like unit was made from the bottom of a 50-mm Polypropylene tube with 28.8mm external diameter and 1.4mm wall thickness (Fisherbrand, Disposable Centrifuge Tube, Fisher Scientific, Leicestershire, UK). The total height of the dome was 17 mm. A 4mm diameter perforation was made in the deepest surface of the dome. A stainless steel tube (65 mm length, 1.5 mm external, 1.1 mm internal diameters) was fitted into a plastic pipette tip

(P50, Clear, 0.5-50 µL, PerkinElmer, MA, USA) with its tip removed to allow the tube to fit and cross from end to end. The dimensions of this precision tip are: 6.56 mm basal external diameter, 2.1 mm distal diameter, 1.6mm internal diameter; after tip removal its length was 40 mm. To improve damping and acoustic radiation, the space between the steel tube and the plastic cast was filled with liquid latex and fitted inside the hole of the dome and fixed using super glue (Loctite®, Chesire, UK). The dome-like unit was then assembled on the loudspeaker cone with boundaries covered with soft silicone for noise reduction (BioEars®, Sandwich Ken, UK). Prior to this step, the internal walls of the dome piece and of the speaker cone inside were lined with a thin lining of cotton wool. This served to reduce reflections inside and improved the power output of the probe loudspeaker. The exposed end of the metallic tube was also covered with liquid latex.

The nominal impedance of the ACR loudspeaker alone was 8 Ω. After fitting the probe unit, acoustic output impedance measured at the probe tip was estimated to be 64.45 Ω, roughly eight times higher. This increase in impedance resulted of course in a reduction of sound pressure: measured at the tip of the probe; however the maximum sound pressure to be obtained was 9.5-10 Pa (~114 dB SPL), using the similar settings in the sound generator as described above.

A calibrated 1/8" B&K microphone was used to cross calibrate the probe loudspeaker's output (4-cycle tones at 23 kHz) at different distances (1-10 mm) away from the probe, assess coherence of acoustic output, and establish that only the probe tip radiates sound. The loudspeaker probe was then mounted on a micromanipulator (World Precision Instruments, Inc., Sarasota, FL, USA) and placed at the spiracle opening. Using the probe, different sound intensities could be accurately played to the spiracle only. For all experiments, the probe was placed at 2 mm from the spiracle. The sound pressure measured at this distance with the 1/8" B&K microphone produced similar tympanal deflections than those obtained with the specimen placed in a free acoustic field and exposed to equivalent sound pressures produced by a normal speaker placed at 30 cm from the preparation. Placing the probe loudspeaker directly at or inside the spiracle, results in over estimation of tympanal vibration. Although several authors have used probe loudspeakers at or inserted into the thoracic spiracles to elicit tympanal vibrations, such procedure is not recommend as it generates large overpressures difficult to quantify

and possibly wave distortion and unwanted nonlinear distortions. The dimensions of the probe loudspeaker used here and the 2 mm distance from the spiracle, provide tympanal defections identical to free-field conditions, and therefore offer a practical alternative method to deliver specific inputs with magnitude and spectral characteristics commensurate with natural signals.

Using these setup and delivery methods, tympanal vibrations were recorded in response to broadband songs (5-50kHz, as described above) and 23 kHz 4-cycle tones delivered at the spiracle were recorded from both ATM and PTM and from the dorsal cuticle using LDV. For broadband sounds, the frequency spectrum of the output of the probe loudspeaker was mathematically equalized using the B&K 3.2 mm precision microphone as a reference placed 2mm away from the probe tip.

Visualization of mechanoreceptors

After removing the dorsal cuticle and exposing the CA surface for laser scans, we stained the exposed surface with Janus Green-B (*23*) in 7 specimens (5 females and 2 males), and viewed it with a dissection microscope (Leica Z12) in mixed transmitted and reflected light). The CA of *C. gorgonensis*, comprises 25 to 28 scolopidia, the multicellular mechanoreceptor units.

Data analysis

Morphological linear measurements of the ear were carried out using the μCT scan reconstruction using the software Amira. Surface areas were calculated from pictures imported into ImageJ. V. 1.42q (Wayne Rasban, National Institutes of Health, USA).

Instantaneous frequencies and phase in the time domain were obtained with Hilbert transform using custom Matlab code (*24*). Travelling waves were obtained from the deflection maps of the FFT analysis resulting from broadband stimulation, but also from the time domain recordings of 4-cycle pure tones at different frequencies (5-50 kHz). Differences in the morphology of the TMs and TPs between males and females were statistically analyzed under a classical *t*-test.

Supplementary Text

Frequency analysis in insects.

In insects, frequency selectivity has been documented at both behavioral and neurobiological levels for several species (*11*, *25*), yet morphological and functional evidence for the supporting biophysical mechanisms is largely missing. In one exceptional case, that of the desert locust, some form of frequency analysis is made possible by the mechanical response of the TM of their abdominal ears. There, frequency analysis is brought about by membrane-borne travelling waves that channel mechanical energy at different, frequency dependent locations on the TM. These locations are where mechanoreceptors capture mechanical energy at selected frequency bands (*19*). This unusual tympanal tonotopy is unique to locusts and allows for incident signal decomposition in only 2 or 3 frequency bands, a simple form of selectivity (*26*). Previous work suggests that katydid ears are more refined than those of the locust in their architecture and capacity for frequency analysis (*8, 10, 13, 27, 28*).

To date, auditory systems performing frequency analysis using dedicated impedance conversion and a fluid-filled dispersive medium have been found only in higher vertebrates. The presence of an auditory system in an insect that employs mammalian-like mechanisms constitutes a remarkable case of convergent evolution. Such convergence demonstrates that auditory sensitivity and frequency analysis are possible for microscale auditory systems, using analogous operating principles yet alternative morphological architecture.

<u>The role of the Auditory Vesicle in the mechanical response.</u>

Additional tests were carried out to document the causal link between the vibrations of the dorsal cuticle and those of the adjacent auditory vesicle (AV), the site of mechanoreception. Ideally, the mechanical coupling between the dorsal cuticle and AV is best measured by a transfer function between their responses. This method requires non-contact vibrometric measurements, which are not directly possible for the AV or CA. Instead, a series of experiments were conducted that test the function of several structures along the chain of hearing, examining the role of the AV. First, the removal of the liquid in the AV by suction through a small proximal hole in the hemolympathic system eliminates all vibrations from the dorsal cuticle. This evidence suggests that vibrations from the intact AV are imparted to the dorsal cuticle. This also implies that in the absence

of functional AV, tympanal vibrations alone are not sufficient to drive the dorsal cuticle (Fig. 4A, and figs. S5 and S6A to G). When one tympanum is removed, and the AV intact, vibrations of the dorsal cuticle are reduced by about half, but not eliminated. Dorsal cuticle vibrations completely disappear when both tympana are ablated (Fig. S5). This indicates that primary and possibly sole input to the AV comes from the tympanal membranes.

These recordings also highlight the role the AV in the process of frequency decomposition and directional wave propagation, confirming our observations obtained from the free-field recordings. All evidence supports the notion that frequency decomposition and wave directionality both arise from the intrinsic mechanical properties of the AV. AV thus fulfills that necessary function, yet might not be sufficient as the likely involvement of the CA and scolopidial mechanosensory units in the overall mechanical response cannot be excluded. Much like in the cochlea of mammalian ears, as frequency decreases vibrations are increasingly localized further along the basilar membrane. Also, waves were observed to always travel in from distal to proximal (Fig. 4C, fig. S6H), confirming results of other researchers on other katydid species, using a different approach (*13*).

Further experiments were conducted to investigate the mechanical contribution of the AV to the overall response of the auditory system. The dorsal cuticle was carefully removed, creating optical access to the AV for LDV measurements (*13*). The vesicle could be then drained of its fluid, a procedure that exposed the anterior tracheal branch containing the *crista acustica* (CA). Moisture of this surface was maintained by applying insect ringer solution using a micropipette, but was subsequently drained during LDV recordings.

Using the acoustic isolation platform (see methods details below, fig. S4B), the probe loudspeaker placed 2 mm clear from the ipsilateral spiracle and LDV, vibrations of the CA surface and of both TMs could be obtained. The isolation platform and probe loudspeaker together guarantee that vibrations recorded from the CA surface are the sole product of acoustic tracheal input to the auditory system, and not of airborne sound reaching the external surface of the CA or other adjacent cuticular structures. A

microphone was placed at the tympanal side to control that airborne sounds do not reach the CA surface (fig. S4B).

Using this methodology, 11 insects (5 females and 6 males) were measured. Three tests were performed; 1. leave the AV intact and record from the dorsal cuticle, 2. drain the AV from its hemolymphatic fluid by opening a small perforation on the cuticle and extracting the fluid with a glass microcapillary tube; 3. remove the cuticle and AV entirely and gain direct optical access to the thin tracheal wall in which the CA is embedded, following the dissection procedure of Palghat Udayashankar et al.(*13*). Vibrometric measurements show that dispersive wave propagation, and therefore frequency decomposition, only occurs in the presence of an intact AV (test 1). All other procedures (tests 2, 3) eliminate traveling waves. Notably, test 3 eliminates travelling waves, contrary to Palghat Udayashankar *et al*. (*13*), yet still shows frequency responses in the CA surface identical to those observed in the intact TM and TP. Travelling waves are also absent in test 2 when AV is drained and vibrations recorded from the dorsal cuticle. Consequently, in *C. gorgnensis* AV is required for the generation of travelling waves across the CA, and therefore the spectral decomposition of incoming mechanical waves.

No frequency decomposition or travelling waves could be observed on the CA surface (fig. S7A). However, the distal 1/4 of the CA surface vibrates in phase with the TPs, but ca. 180 out of phase with respect to the TMs (Fig. S7A, C). Similar results were obtained with pure tone stimulation (fig. S7B). This evidence shows that the transmission of mechanical energy remains intact in this procedure, yet only dispersive propagation is disrupted (fig. S7C). When both TMs are removed, however, CA vibrations vanish, suggesting that CA vibrations are induced by TMs via the TPs.

At the regular specific sound pressures a female is exposed in nature , only the 1/4 distal part of the anterior tracheal branch containing the CA vibrates when both TMs respond to sound delivered to the spiracle only (using the isolating platform, test 3). This is different to what Palghat Udayashankar *et al*. (*13*) observed from measurement made in non-intact conditions directly on the CA surface of the katydid *Mecopoda elongata*. Travelling waves were observed that are similar to those reported here, propagating from distal to proximal. This establishes that the tracheal support to the CA vibrates in

response to sound in this species. Notably in *C. gorgonensis*, the tympanal mechanical response to 4-cycle tones at 23 kHz is not affected by invasive procedures (our tests 2-3) and the 180° phase inversion between TM and CA remains intact (fig. S3). However, the procedures used in our tests 2 and 3 cause the loss of the travelling waves. Instead, the distal most part of the CA moves using a single, non-dispersive mode for all frequencies, with deflections strictly in phase with those of the TP (fig. S3).

Altogether, this evidence suggests that the AV receives direct input from the TP feeding into the narrowest and most distal part of the tracheal division supporting the CA. These results also indicate that the AV, the fluid within it and the anisotropic substrate offered by the CA are necessary for the build up of the spectral decomposition of the incoming vibrations. Because TP behavior is not affected, it can be concluded that impedance conversion and frequency decomposition are independent processing stages.

An additional line of evidence documenting the presence of travelling waves along the dorsal cuticle and the auditory vesicle is provided by the FFT- based topographical reconstruction of deflection shapes. Measured in response to frequency sweeps (5-50 kHz) delivered in free-field, the travelling waves invariably start at the distal end of the dorsal cuticle, where high frequency resonances occur (as seen in Fig 4. A P6-7) and move towards the proximal end of the FV. How far the wave then travels depends on frequency of the incoming sound (Fig. 4E). The deflection shapes elicited by high frequency sound input do not travel far along the cuticle, while low frequency-elicited mechanical waves spread some 400 μm further to the proximal end of the dorsal cuticle. This phenomenology is identical to that of the cochlear frequency analyzer of mammals, as first shown by Georg von Békésy.

At any of the frequencies contained in the frequency sweep, a travelling wave is generated that invariably starts at the distal end of the dorsal cuticle and CA and migrates towards the proximal end of the AV. The lower the frequency of the incoming sound, the further the wave travels along the AV (fig. S6, movie S3). The dispersive nature of such wave propagation is documented by the accumulation of phase delays that are frequency and place dependent (Fig. 4C).

<u>Anatomy and composition of the auditory vesicle</u>

The μCT scans reveal that the AV is not a continuation of the tibial hemolymphatic vessel (fig. S2), but is structured as a distinct compartment with only a thin proximal connection to the hemolymphatic system. This anatomy was also observed across 4 different species of 4 different subfamilies [*Arachnoscelis* sp. (Listroscelidinae), *Metrioptera sphagnorum* (Tettigoniinae), *Panacanthus pallicornis* (Copiphoninae), and *Parascopioricus cordillericus* (Pseudophyllinae)]. The distal end of the auditory vesicle is blind, and in some species it is as narrow as the distal end of the CA surface (see Movie S1). Both ends of the AV are occupied by a small plug of colloidal material that is distinct from the fluid seen in the AV's middle section. The role of the plug material in the hearing process remains unknown, yet speculatively we suggest it may help dissipating acoustic energy towards the ends of the AV and/or maintaining a constant volume of fluid within the AV. From μCT scans, a thin membrane delimiting the AV from the surrounding tissue can be observed, which is also evident in histological work done by others (e.g., (*29*)). The proximal and distal ends of the vesicle are thus surrounded by non-hemolymphatic tissue, while most of its dorsal surface is directly adjacent to the cuticular epidermis.

Apolar extraction using cyclohexane, indicates that the AV fluid contains lipids. AV fluid is completely soluble in cyclohexane, while extractions of liquid from the adjacent hemoplymphatic channel are not. The ultrastructural histology and proper chemical characterization of the AV constitute promising avenues of research, as the involvement of oily substances in arthropod audition now appears to be necessary to frequency processing.

<u>The impedance converter as part of the tympanal system.</u>

Bangert et al. (*8*), using single point LDV, suggested an impedance-matching function for the tympana and described the tympanal vibrations as being similar to that of a plate moving around a hinge. These authors saw the tympanum hinged around the dorsal cuticle of the leg. In that study, there is no anatomical or mechanical evidence of mobile TPs on the dorsal part of the tympanum. In the functional explanation by Bangert et al. (*8*) , the excitation of the mechanoreceptors is achieved when both tympana deflect and deform the dorsal wall of the trachea containing the AC, and causes a 'negative pressure' in the hemolymph channel by expanding its cavity (see figure 9 in their paper). In a more

recent study, using microscanning LDV, Palghat Udayashankar *et al*. (*13*) show travelling waves recorded from the dorsal surface of the trachea containing the CA. Bangert's et al. (*8*) data and hinge model suggest that sound is not transmitted from the air medium to a liquid medium, but vibration transmission to the CA is direct. Both studies (*8,13*) on two phaneropterine and one Tettigoniinae katydids show no evidence of an impedance conversion mechanism or dispersive medium (fluid-filled vesicle). One interesting next step is to investigate the detailed internal anatomy of several katydid species across different subfamilies to understand the morphological and functional diversity of auditory mechanisms, with special focus on impedance conversion.

As a key step in the chain of hearing, impedance conversion is supported by unconventional morphology in *C. gorgonensis*. The TM and TP together constitute a remarkable micromechanical system. When driven by acoustic pressure, this system generates a rocking behavior, whereby a large outward displacement of the TM is accompanied by a smaller, inward, displacement of the TP. The pattern of vibration revealed by the scanning laser Doppler measurements and their topographical mapping gives insight into the function of this system. Morphologically TM and TP are linked but are distinct structures. TM is a thin (6-16 μm) membrane which presents both sides to air, while TP is thicker (20-30μm), has one side facing air and the other applied to the fluid of AV (fig. S8). In terms of surface area, TM is 360-465 μm^2, and TP is 28-35 μm^2 a surface ratio of nearly 13 (Table S1). TM morphology also exhibits specializations not seen in other tympanal insects and likely unique to the katydid system. The cuticle between TM and TP is a rigid dense ridge that serves as a fulcrum. Only the portion of TM perimeter adjoining TP has this particular anatomy. The contour of the TM differs from other insects (e.g., grasshoppers, weta, field and tree crickets and grigs (*22, 30-32*)) as it is distinctly kidney shaped. We propose that this specific and unusual tympanal shape serves to channel vibrational energy to the AV via the TP, a notion supported by our early finite element analysis. In effect, kidney shaped TMs in some but not all katydid species may be the hallmark of impedance conversion and frequency analysis.

It is interesting to note here that both anterior and posterior TMs are associated with a TP (fig. S8). Hence both TPs contribute to efficiently driving mechanical energy into the AV and auditory organ proper. Data show that both TMs vibrate in phase, as well as both

TPs (but TPs and TMs vibrating in antiphase). The ablation of one TM is also shown to reduce the vibrations of the AV by about half, while removal of both TMs eliminates AV vibrations altogether, as recorded from dorsal cuticle. This evidence suggests that the presence of two TMs contributes to enhance the overall sensitivity of the ear, doubling the mechanical input.

Supporting references and notes (full reference list included at the end of this file)

21. S. Goutte, N. M. Kime, T. F. Argo IV, M. J. Argo, Calling strategies of male tungara frogs in response to dynamic playback. *Behaviour* **147**, 65 (2010).
22. N. Mhatre, F. Montealegre-Z, R. Balakrishnan, D. Robert, Mechanical response of the tympanal membranes of the tree cricket *Oecanthus henryi*. *J. Comp. Physiol. A Neuroethol. Sens. Neural Behav. Physiol.* **195**, 453 (2009).
23. J. E. Yack, Janus Green-B as a rapid, vital stain for peripheral nerves and chordotonal organs in insects. *J Neurosci Methods* **49**, 17 (1993).
24. W. H. Hartmann, *Signals, Sound and Sensation* (Springer Verlag, New York, 1998).
25. H. Römer, in *Acoustic and Vibrational Communication in Insects,* K. Kalmring, N. Elsner, Eds. (Paul Parey, Berlin, 1985), pp. 25-32.
26. N. H. Fletcher, *Acoustic Systems in Biology* (Oxford University Press, Oxford, 1992).
27. W. Roessler, M. Jatho, K. Kalmring, in *Insect Sounds and Communication: Physiology, Behaviour, Ecology and Evolution,* S. Drosopoulos, M. Claridge, Eds. (Taylor & Francis, London, 2006), pp. 35-69.
28. R. Schumacher, Morphologische Untersuchungen der tibialen Tympanalorgane von neun einheimischen Laubheuschrecken-Arten (Orthopter, Tettigonioidea). *Z. Morphol. Tiere* **75**, 267 (1973).
29. W. Rossler, A. Hubschen, J. Schul, K. Kalmring, Functional morphology of bush-cricket ears: Comparison between 2 species belonging to the Phaneropterinae and Decticinae (Insecta, Ensifera). *Zoomorphology* **114**, 39 (1994).
30. K. Lomas, F. Montealegre-Z, S. Parsons, L. H. Field, D. Robert, Mechanical filtering for narrow-band hearing in the weta. *J. Exp. Biol.* **214**, 778 (2011).
31. A. C. Mason, Hearing in a primitive Ensiferan: The auditory system of *Cyphoderris monstrosa* (Orthoptera, Haglidae). *J. Comp. Physiol. A Neuroethol. Sens. Neural Behav. Physiol.* **168**, 351 (1991).
32. D. Robert, in *Sound Source Localization,* A. N. Popper, R. R. Fay, Eds. (Springer-Verlag New York, 2005), vol. 25, pp. 6-35.

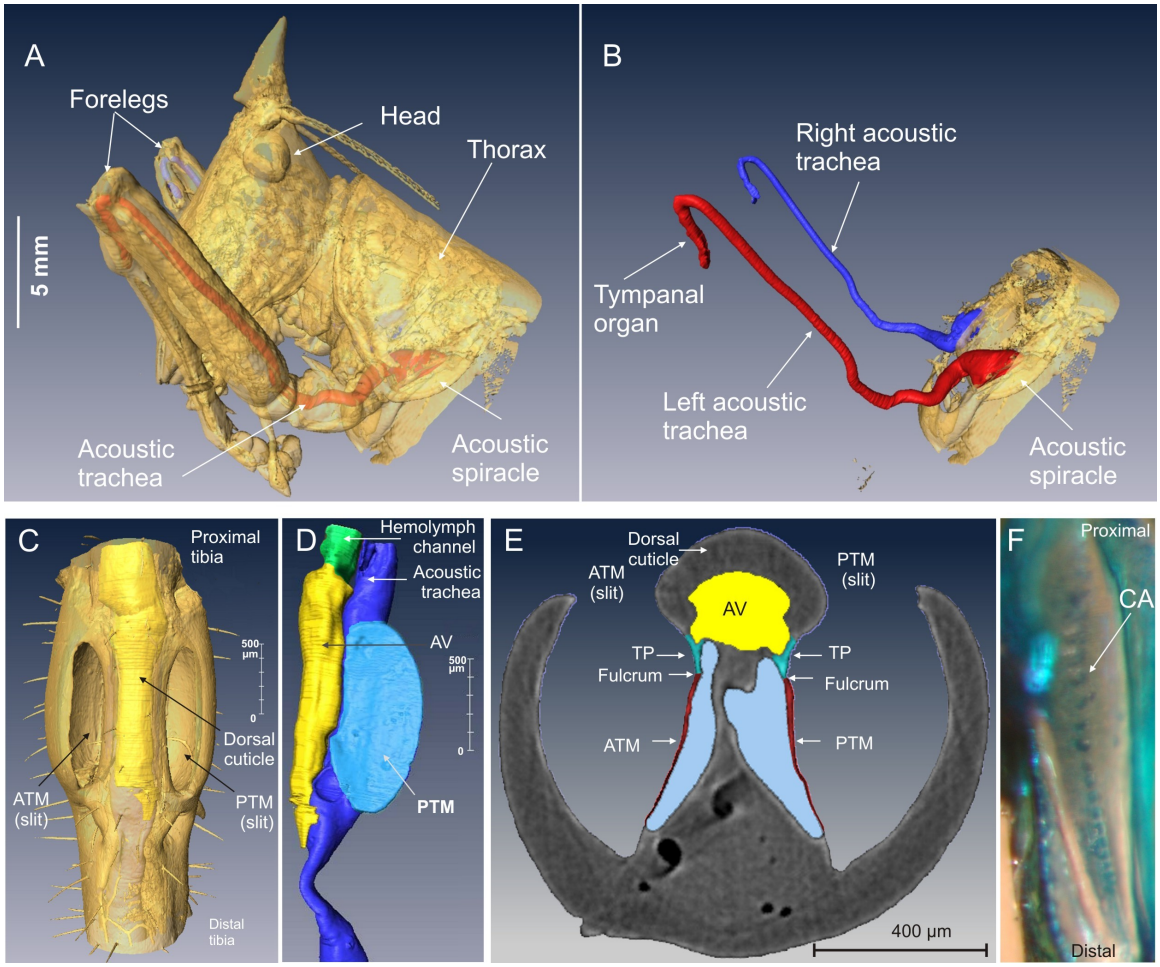

Fig. S1.

Micro CT X-ray 3D reconstruction of the ear of *Copiphora gorgonensis*. (**A**) The acoustic trachea of a female (blue and red tubes), seen *in situ* through semi-transparent cuticle. (**B**) Cuticle and surrounding tissue removed digitally to reveal tracheal layout and location of tympanal organ. (**C**) View of male proximal tibia and tympanal organ, showing the position of the auditory vesicle (yellow, AV) underneath the dorsal cuticle. (**D**) 3-D reconstruction of the auditory system with acoustic trachea (dark blue), posterior tympanal membrane (PTM, light blue), tympanal plate (TP, light green), fluid vesicle (yellow), and hemolymph channel (green). (E) Opened foreleg tibia showing CA after staining with Janus green B.

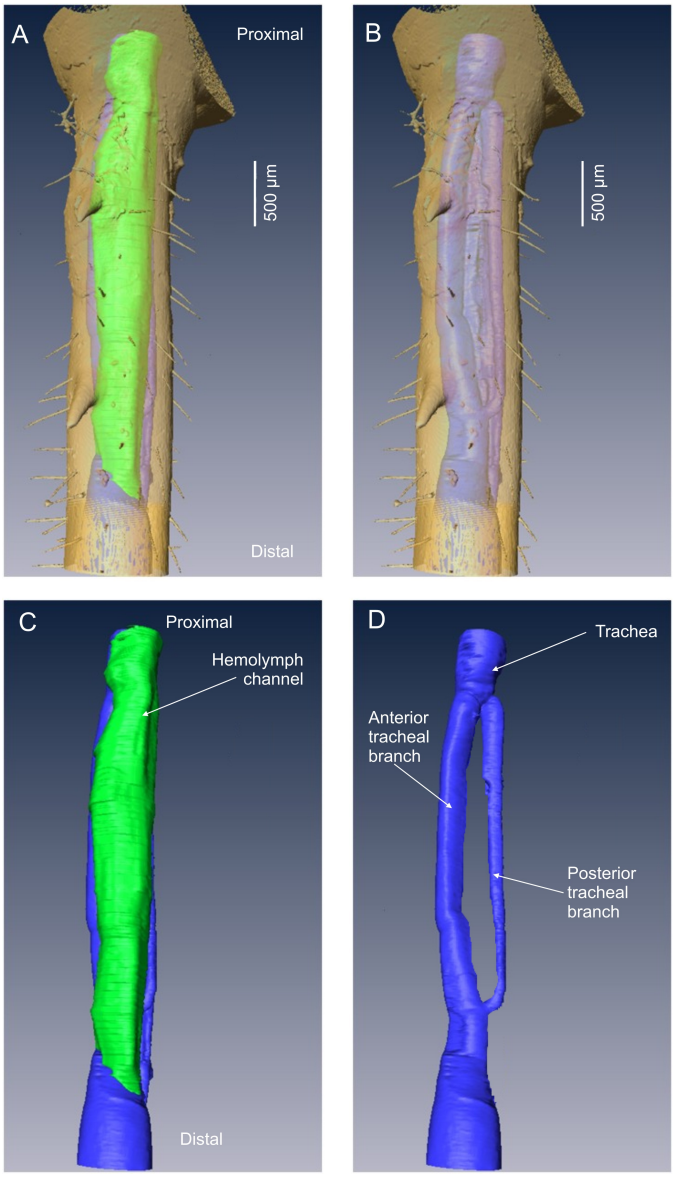

Fig. S2.

Anatomy of the earless mesothoracic right tibia of a female *C. gorgonensis* (µCT reconstruction). (**A, B**) external views of the tibia with semi-transparent cuticle showing hemolymph channel (green) and trachea (blue). (**C, D**) Digital removal of tibial cuticle reveals the hemolymph channel (green) and two tracheal branches (blue). Auditory specializations, such as the tympanum, fluid vesicle and acoustic trachea are absent. The hemolymph channel is a continuous blood vessel irrigating femur and tibia. Notably, the trachea divides in two branches that do not exhibit tympanal expansions.

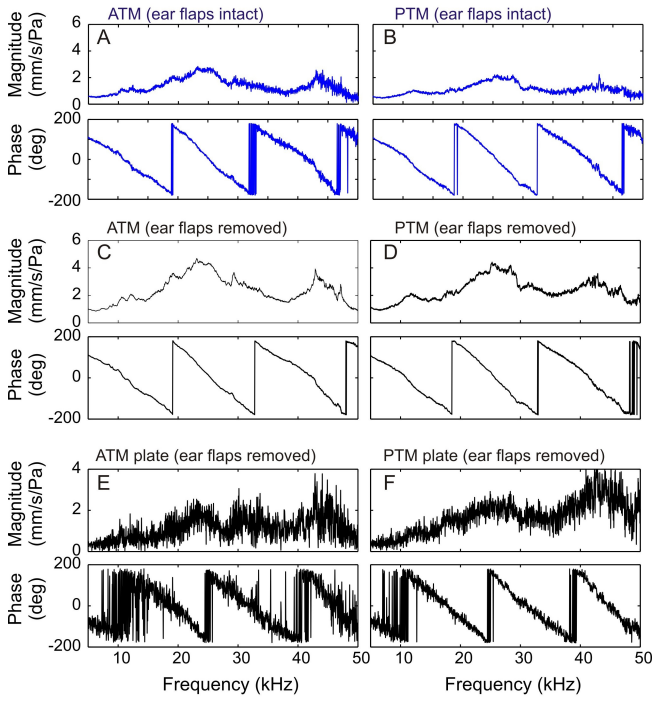

Fig. S3.

Frequency response transfer functions of the female tympanal membranes (ATM and PTM) and their respective tympanal plates (TP) to broadband acoustic stimulation (5-50kHz). (**A, B**) ATM and PTM magnitude and phase spectra obtained with tympanal flaps intact. (**C, D**) ATM and PTM magnitude and phase spectra obtained with tympanal flaps removed. (**E, F**) ATM and PTM plates magnitude and phase spectra. No frequency selection is present at TMs or TPs. Phase spectra reveal a phase difference of 180° between TMs and TPs for all frequencies tested.

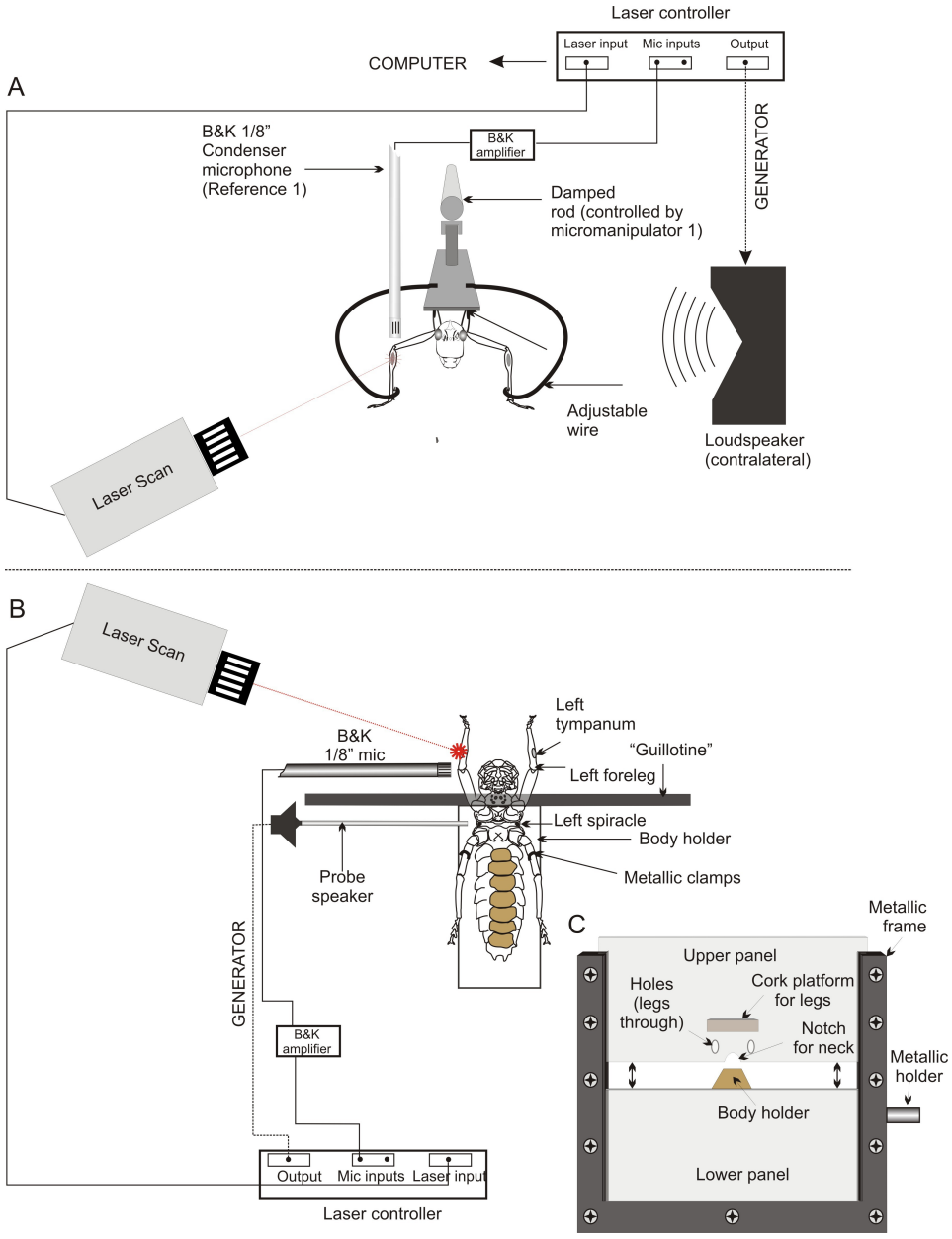

Fig. S4.

Experimental setups for controlled sound delivery and laser recordings of the katydid ears. (**A**) Free-field ear stimulation with the intact insect mounted to a holder. (**B**) Tracheal acoustic stimulation using a probe loudspeaker. Sound can be delivered to the acoustic spiracle only, precluding any sound pressure from reaching the tympana or the leg cuticle. This setup allowed the demonstration that vibrations of the AV recorded though the cuticle are not the product of artifactual leg resonances due to tethering. Drawings are not to scale.

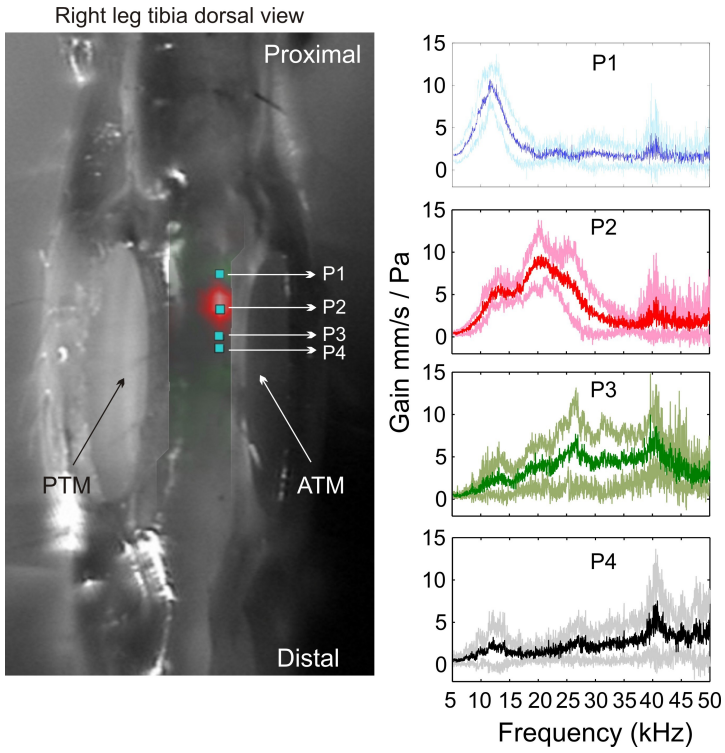

Fig. S5.

Average frequency response of the dorsal cuticle in males and females *C. gorgonensis*. Vibrations recorded through the dorsal cuticle. Left panel shows a close view of the posterior tympanal area, and the deflection map (in green and red colors) of the dorsal cuticle. P1–P4 blue square dots show the locations from which frequency spectra were measured for 21 animals. The four right panels depict the frequency responses at said locations (n=21, 11 females and 10 males, ±1SD). High frequencies predominate distally (P4) while low frequencies do so proximally (P1). Sound stimuli were produced using the acoustic setup described in Fig. S4B.

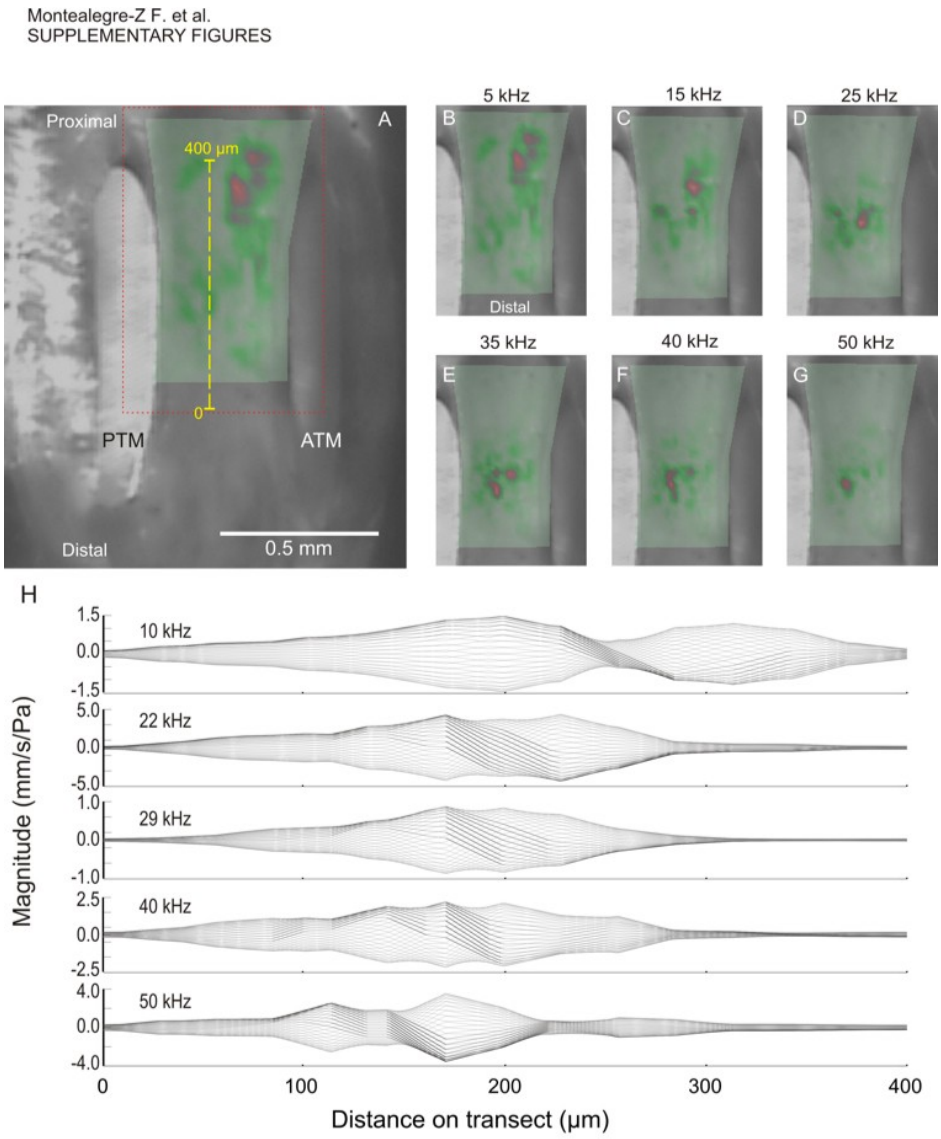

Fig. S6.

Vibration map of the dorsal cuticle of the tympanal organ produced by FFT analysis. Tympanal vibrations were elicited by broadband frequency sweep stimuli (5-50kHz). (**A**) The right tibia ear, with vibration deflection map superimposed. (**B-G**) Close-up views of the red dashed area are showing the spatial distribution of cuticular vibrations (red spots) for different driving frequencies. The width of the band of each of the analytical frequencies represented in the panels was 31.8 Hz. The vibration map clearly shows that high frequency vibrations are located distally, while low frequencies occur proximally. (**H**) Envelopes of mechanical deflections on the cuticle along the transect line in A, for different driving frequencies.

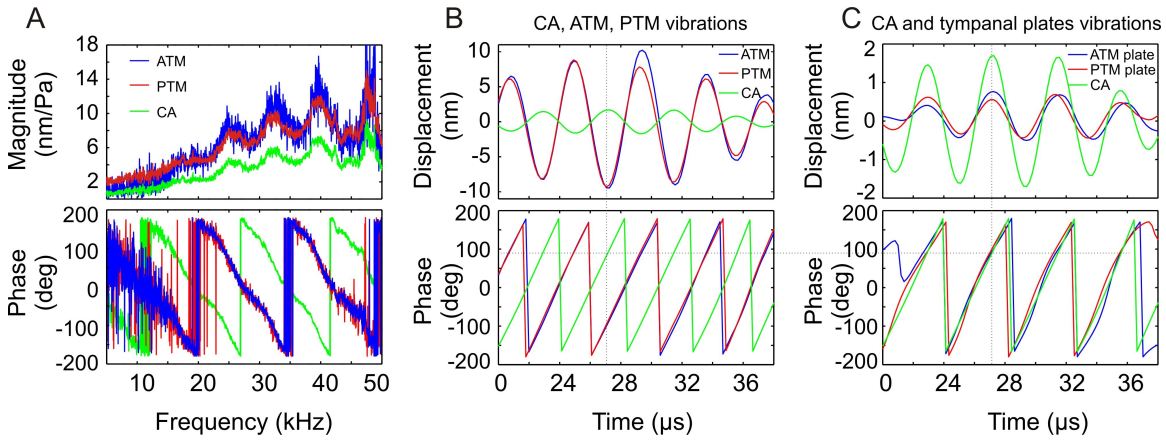

Fig. S7.

Mechanical response of tympanal system and sensory organ (*crista acustica*). (**A**) Frequency spectrum magnitude and phase transfer function of ATM, PTM and CA after removal of the hemolymphatic fluid and exposing the CA. Broadband acoustic stimulus was delivered using the preparation in Fig. S4B. ATM, PTM and CA mechanical responses are similar, revealing the loss of frequency decomposition at the CA surface. The phase spectra indicate a phase difference of 180° between tympanum and CA surface, because coupling between them is not affected. (**B**) Time-resolved responses of ATM, PTM and CA to a pure tone stimulus (a 23kHz, 4-cycle sound pulse). Lower panel shows the phase of the oscillations determined by Hilbert transform. ATM and PTM oscillate in phase, while CA response is clearly 180° out of phase, supporting the FFT analysis shown in A. (**C**) Time-resolved oscillations of ATM and PTM plates and the CA to 23kHz. All elements oscillate in phase, confirming the coupling between tympanal plates and CA.

Table S1. Group statistics and mean comparison tests for tympanal dimensions in males and females

Males	Mean (μm)	N	Std	**Females**	Mean (μm)	N	Std
Male ATM	356.75	10	16.33	Female ATM	463.63	11	68.04
Male ATM plate	28.05	10	3.26	Female ATM plate	35.74	11	3.69
Male ATM/TP ratio	12.83	10	1.13	Female ATM/TP ratio	12.94	11	1.17

t-test for equity of means

	t	df	Sig (2-tailed)	SE
Female ratio vs Male ratio	0.23	19	0.826	0.503
Female ATM vs Male ATM	5.138	19	0.000	0.022
Female TP vs Male TP	5.178	19	0.000	0.016

Supplementary movie captions

Caption for Movie S1: 3-D reconstruction of the internal organization of the tympanal organ in left tibia of a female *Panacanthus pallicornis* (Orthoptera: Tettigoniidae: Copiphorini). The animation highlights the morphological difference between the fluid-filled auditory vesicle and hemolymphatic channel. These two structures are clearly separated by a narrow joint.

Caption for Movie S2: Tympanal mechanics and impedance conversion in the anterior tympanic membrane of *Copiphora gorgonensis* (Orthoptera: Tettigoniidae: Copiphorini). The video illustrates the rocking motion of the tympanum and tympanal plate at 23kHz. Similar motion is observed at other frequencies as well.

Caption for Movie S3: Time-resolved mechanical response to 23kHz 4-cycle tone. The video illustrates a wave travelling across the transect shown in the video-feed picture. The yellow dot in the picture represents a landmark on the proximal part of the dorsal cuticle. This position is indicated in the animated longitudinal section by the vertical yellow line. Notable waves travel in direction distal to proximal.

References and Notes

1. W. Bialek, Physical limits to sensation and perception. *Annu. Rev. Biophys. Biophys. Chem.* **16**, 455 (1987). doi:10.1146/annurev.bb.16.060187.002323 Medline

2. A. J. Hudspeth, How the ear's works work. *Nature* **341**, 397 (1989). doi:10.1038/341397a0 Medline

3. G. von Békésy, *Experiments in Hearing* (McGraw-Hill, New York, 1960).

4. J. Ashmore, Cochlear outer hair cell motility. *Physiol. Rev.* **88**, 173 (2008). doi:10.1152/physrev.00044.2006 Medline

5. L. Robles, M. A. Ruggero, Mechanics of the mammalian cochlea. *Physiol. Rev.* **81**, 1305 (2001). Medline

6. F. Montealegre-Z, M. Postles, Resonant sound production in *Copiphora gorgonensis* (Tettigoniidae: Copiphorini), an endemic species from Parque Nacional Natural Gorgona, Colombia. *J. Orthoptera Res.* **19**, 347 (2010). doi:10.1665/034.019.0223

7. J. E. Yack, The structure and function of auditory chordotonal organs in insects. *Microsc. Res. Tech.* **63**, 315 (2004). doi:10.1002/jemt.20051 Medline

8. M. Bangert *et al*., Stimulus transmission in the auditory receptor organs of the foreleg of bushcrickets (Tettigoniidae) I. The role of the tympana. *Hear. Res.* **115**, 27 (1998). doi:10.1016/S0378-5955(97)00177-9 Medline

9. D. B. Lewis, The physiology of the tettigoniid ear. II. The response characteristics of the ear to differential inputs: lesion and blocking experiments. *J. Exp. Biol.* **60**, 839 (1974). Medline

10. K. Kalmring, W. Rossler, R. Ebendt, J. Ahi, R. Lakes, The auditory receptor organs in the forelegs of bush-crickets: Physiology, receptor cell arrangement, and morphology of the tympanal and intermediate organs of 3 closely related species. *Zool. Jahrb. Allg. Zool.* **97**, 75 (1993).

11. B. P. Oldfield, Tonotopic organization of auditory receptors in Tettigoniidae (Orthoptera, Ensifera). *J. Comp. Physiol.* **147**, 461 (1982). doi:10.1007/BF00612011

12. R. R. Hoy, D. Robert, Tympanal hearing in insects. *Annu. Rev. Entomol.* **41**, 433 (1996). doi:10.1146/annurev.en.41.010196.002245 Medline

13. A. Palghat Udayashankar, M. Kössl, M. Nowotny, Tonotopically arranged traveling waves in the miniature hearing organ of bushcrickets. *PLoS ONE* **7**, e31008 (2012). doi:10.1371/journal.pone.0031008 Medline

14. Materials and methods are available as supplementary materials on *Science* Online.

15. M. Nowotny, J. Hummel, M. Weber, D. Möckel, M. Kössl, Acoustic-induced motion of the bushcricket (*Mecopoda elongata*, Tettigoniidae) tympanum. *J. Comp. Physiol. A Neuroethol. Sens. Neural Behav. Physiol.* **196**, 939 (2010). doi:10.1007/s00359-010-0577-6 Medline

16. R. Boistel *et al*., Whispering to the deaf: Communication by a frog without external vocal sac or tympanum in noisy environments. *PLoS ONE* **6**, e22080 (2011). doi:10.1371/journal.pone.0022080 Medline

17. J. Mueller, L. A. Tsuji, Impedance-matching hearing in Paleozoic reptiles: Evidence of advanced sensory perception at an early stage of Amniote evolution. *PLoS ONE* **2**, e889 (2007).

18. H. A. Thomassen *et al*., Do swiftlets have an ear for echolocation? The functional morphology of swiftlets' middle ears. *Hear. Res.* **225**, 25 (2007). doi:10.1016/j.heares.2006.11.013 Medline

19. J. F. C. Windmill, M. C. Göpfert, D. Robert, Tympanal travelling waves in migratory locusts. *J. Exp. Biol.* **208**, 157 (2005). doi:10.1242/jeb.01332 Medline

20. J. J. Belwood, G. K. Morris, Bat predation and its influence on calling behavior in neotropical katydids. *Science* **238**, 64 (1987). doi:10.1126/science.238.4823.64 Medline

21. S. Goutte, N. M. Kime, T. F. Argo IV, M. J. Argo, Calling strategies of male tungara frogs in response to dynamic playback. *Behaviour* **147**, 65 (2010). doi:10.1163/000579509X12483520922205

22. N. Mhatre, F. Montealegre-Z, R. Balakrishnan, D. Robert, Mechanical response of the tympanal membranes of the tree cricket *Oecanthus henryi*. *J. Comp. Physiol. A Neuroethol. Sens. Neural Behav. Physiol.* **195**, 453 (2009). doi:10.1007/s00359-009-0423-x Medline

23. J. E. Yack, Janus Green B as a rapid, vital stain for peripheral nerves and chordotonal organs in insects. *J. Neurosci. Methods* **49**, 17 (1993). doi:10.1016/0165-0270(93)90105-Z Medline

24. W. H. Hartmann, *Signals, Sound and Sensation* (Springer, New York, 1998).

25. H. Römer, in *Acoustic and Vibrational Communication in Insects*, K. Kalmring, N. Elsner, Eds. (Paul Parey, Berlin, 1985), pp. 25–32.

26. N. H. Fletcher, *Acoustic Systems in Biology* (Oxford Univ. Press, Oxford, 1992).

27. W. Roessler, M. Jatho, K. Kalmring, in *Insect Sounds and Communication: Physiology, Behaviour, Ecology and Evolution*, S. Drosopoulos, M. Claridge, Eds. (Taylor & Francis, London, 2006), pp. 35–69.

28. R. Schumacher, Morphologische untersuchungen der tibialen tympanalorgane von neun einheimischen laubheuschrecken-arten (Orthopter, Tettigonioidea). *Z. Morphol. Tiere* **75**, 267 (1973). doi:10.1007/BF00288474

29. W. Rössler, A. Hübschen, J. Schul, K. Kalmring, Functional morphology of bush-cricket ears: Comparison between 2 species belonging to the Phaneropterinae and Decticinae (Insecta, Ensifera). *Zoomorphology* **114**, 39 (1994). doi:10.1007/BF00574913

30. K. Lomas, F. Montealegre-Z, S. Parsons, L. H. Field, D. Robert, Mechanical filtering for narrow-band hearing in the weta. *J. Exp. Biol.* **214**, 778 (2011). doi:10.1242/jeb.050187 Medline

31. A. C. Mason, Hearing in a primitive ensiferan: The auditory system of *Cyphoderris monstrosa* (Orthoptera, Haglidae). *J. Comp. Physiol. A Neuroethol. Sens. Neural Behav. Physiol.* **168**, 351 (1991). doi:10.1007/BF00198354

32. D. Robert, in *Sound Source Localization*, A. N. Popper, R. R. Fay, Eds. (Springer, New York, 2005), vol. 25, pp. 6–35.